



Fabrication of nickel filter by uniaxial pressing process for gas purification: ceramic coating effect for hot gas cleaning

Shin-Kun Ryi, Kyung-Ran Hwang, Jong-Soo Park*

Reaction and Separation Material Research Center, Korea Institute of Energy Research, 102 Gajeong-ro, Yuseong-gu, Daejeon 305-343, South Korea
Email: deodor@kier.re.kr

Received 3 September 2010; Accepted 3 January 2011

ABSTRACT

A nickel filter for hot gas cleaning was successfully fabricated by pressing micron-size nickel powder. The deposition of the alumina coating on nickel powder having a particle size distribution of 2 to 10 μm is the first step in the fabrication procedure. The raw nickel powder and alumina modified nickel powder were pressed in a cylindrical metal mold under a pressure of 42 MPa and then heat treated in the temperature ranges of 450–900°C and 1100–1400°C, respectively, for 10 h in pure hydrogen to endow them with thermal stability and mechanical strength. SEM, mercury porosimetry and the air permeation test showed that the alumina coating on the surface of the nickel powder hindered the sintering and agglomeration of nickel up to 1200°C, while the pore structure of the un-modified nickel filter was destroyed at 550°C. We believe that the nickel filter developed herein could be applied not only to high temperature processes, such as solid fuel gasification for the reliable and environmentally sound operation of subsequent processes, but also provide energy savings and more effective whole process optimization.

Keywords: Filter; Hot gas cleaning; Nickel powder; Pressing; Alumina coating

1. Introduction

High temperature gas cleaning is one of the most promising technologies, because it can potentially achieve substantial energy savings and provide more effective whole process optimization. This means that the installation of a high temperature gas cleaning process can protect the subsequent parts of the system, such as condensation equipment, heat exchangers and/or wet scrubbers. Some potentially applicable processes for high temperature gas cleaning are shown in Table 1.

Among these processes, the gasification process for solid fuels, such as coal, biomass and waste, has attracted a great deal of attention, because of the recent increase in the price of oil and (the problems posed by °C) greenhouse

gases. The gas produced by the solid fuel gasification process consists of hydrogen, carbon monoxide and hydrocarbons and can be used as a fuel in molten carbonate fuel cells (MCFCs) and gas turbines or as a raw material for the synthesis of hydrocarbons, i.e., methanol, liquefied petroleum gas (LPG), gasoline, etc. [15–19]. However, apart from the main gas components, i.e., N_2 , H_2 , CO , CO_2 , H_2O and CH_4 , the product gas from the gasifier contains several impurities, such as particles, tars, alkalis (Na, K), nitrogen compounds and sulfur compounds. [2,15,20,21]. The particles are especially likely to result in plugging, the abrasion of downstream equipment and environmental pollution. Even though a large portion of these particles are of micron size in terms of their mass distribution, the number of sub-micron size particles is quite high. Thorough gas cleaning of the gasification gas is therefore essential for reliable and environmentally sound operation [22].

*Corresponding author.

Table 1
Potentially applicable processes for high temperature gas cleaning

Industry	Process	Temperature [°C]	Ref.
Power generation	Coal combustion	Up to 1,500	[1]
	Gasification	Up to 1,450	[2][3]
Waste handling	Incineration/gasification	Up to 1,200	[4][5][6]
Chemical process	Catalytic cracking	200–600	[7][8]
	Calcination/drying	Up to 1,300	[9]
	Particle production in the gas phase (e.g., TiO ₂ , SiO ₂)	Up to 1,400	[10][11]
	Metal-roasting and Smelting	Up to 1,000	[12]
Metal-processing industry	Metal-roasting and Smelting	Up to 1,000	[12]
Ceramic industry	Glass/ceramic production	Up to 1,200	[13]
Motor vehicle	Diesel particulate filter (DPF)	600–700	[14]

There are different kinds of filter media. While fine pore size ceramic media are available for use at high temperature [23,24], ceramic filters have some limitations, i.e., weak mechanical strength, long-term microstructural instabilities under the operating conditions of temperature and vapor, and permeability limitations. On the other hand, metal filters have potential advantages, such as good handling, mounting and sealing properties and the ability to withstand the thermo-mechanical shocks and stress caused by system vibration [25]. These filters can be cleaned in situ by back pulsing, washing with water or other methods. Unfortunately, metal filters cannot remove the ultrafine particles in the sub-micron size range from the gases introduced into the solid fuel gasification process.

In our previous paper, we showed that nickel filters could separate sub-micron size NaCl particles with a very high separation efficiency [26]. The aim of this study is to increase the sustainable temperature of nickel filters used to separate ultrafine particles from gas with high efficiency. Coating alumina on the nickel powder, pressing in a cylindrical metal mold, and sintering were used to manufacture this kind of high efficiency nickel filtering media. The gas permeation test based on the pressure difference was carried out with air at room temperature. The nickel and alumina modified nickel filters were characterized by SEM and mercury porosimetry.

2. Experimental

2.1. Fabrication of nickel and alumina modified nickel filtering media

A pure nickel powder purchased from Chang-Sung corp. with a purity of 99.9% and particle size distribution from 2 to 10 μm was coated with aluminum nitrate solution by the incipient wetness impregnation method. An appropriate amount of aluminum nitrate (Al(NO₃)₃·9H₂O, Aldrich) was dissolved in deionized water and the solution was added to the dried nickel powder to obtain 0.5 wt.% Al. The alumina modified nickel powder was then

dried in a convection oven (120°C) for 4 h and calcined at 400°C for 4 h. 15 g of the raw and alumina modified nickel powders were compressed without a binder in a metal cylindrical mold with a diameter of 50 mm using a homemade press under a pressure of 42 MPa. The compressed nickel filters and alumina modified nickel filter were further heat treated in a vacuum furnace filled with high-purity hydrogen. The temperature ranges of the nickel filter and alumina modified nickel filter were 450–900°C and 1100–1400°C, respectively. The thickness of the prepared nickel filters was around 1.5 mm. Table 2 lists the fabrication conditions of the nickel filters (designated as the CN series) and alumina modified nickel filters (designated as the AC series). SEM analysis was used to examine the surface properties of the nickel and alumina modified nickel filters. The average pore size, total pore volume and porosity of the prepared filters were measured by mercury porosimetry (Micromeritics, Autopore °C 9500).

Table 2
The fabrication conditions and thickness of the nickel nano-filter

Filter	Fabrication pressure [MPa]	Heat treatment temperature [°C]
CN042045	42	450
CN042050	42	500
CN042055	42	550
CN042060	42	600
CN042065	42	650
CN042070	42	700
CN042080	42	800
CN042090	42	900
AC042110	42	1100
AC042120	42	1200
AC042130	42	1300
AC042140	42	1400

CN: Nickel powder;

AC: Alumina coated nickel powder.

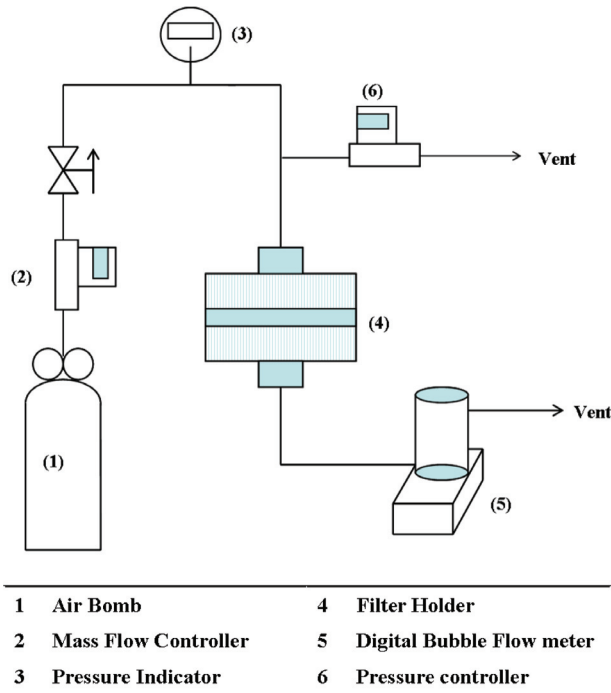


Fig. 1. Schematic diagram of air permeation apparatus.

2.2. Gas permeation test

The gas permeation test was conducted with air at temperatures in the range from room temperature to 700°C. The permeation apparatus consisted of a filter assembly, pressure indicator, mass flow controller and digital bubble flow meter, as shown in Fig. 1. Air was introduced by a mass flow controller (MCF, Brooks 5850 E series) and the pressure was detected by a digital pressure regulator (Alicat, PC-30PSIG-D). The air permeation flux was measured by a digital soap-bubble flow meter (SENSIDYNE, Gilibrator 2). The filter was inserted in the filter holder and fastened to the holder by a Viton O ring for use at room temperature and a metal O ring for use at high temperatures.

3. Results and discussion

3.1. Filter properties

In previous studies, we showed that the gas permeation decreased with increasing fabrication pressure [26]. This means that the fabrication pressure is one of the most important means of increasing the air permeation. On the other hand, heat treatment improves the mechanical strength and thermal resistance of the filter. However, small sized metal powders are prone to be sintered at high temperature. This causes the porosity, average pore diameter and total pore volume of the filter, as well as the air permeation flux, to decrease. In order to clarify the effect of the heat treatment temperature, the CN

series and AC series filters were treated in the temperature ranges of 450–900°C and 1100–1400°C, respectively. Fig. 2 shows the SEM images of the CN and AC series nickel filters. Since it underwent sintering from 600°C (CN042060), the undulating surface of the raw nickel powder became smooth. Furthermore, above 700°C (CN042070), the pore fraction drastically decreased with increasing heat treatment temperature. On the other hand, the AC series filters showed a very stable structure up to 1200°C (AC042120). At 1300°C (AC042130), the filter partly melted and some pores became plugged. At 1400°C (AC042140), the majority of the filter melted and most of the pores became plugged.

In Fig. 3, the porosity and average pore diameter of the CN (a) and AC (b) series filters are shown as a function of the heat treatment temperature. As shown in this figure, the porosity of the CN series filters increased as the heat treatment temperature increased from 450 to 500°C and then decreased as the heat treatment temperature was further increased. On the other hand, the average pore diameter of the CN series filters increased as the heat treatment temperature increased from 450 to 550°C and then decreased as the heat treatment temperature was further increased. The surface sintering of nickel powder at 550°C extends its pore size and seems to cause the porosity and average pore diameter to increase. However, above 550°C, the nickel powder melts and its pores become plugged, resulting in a decrease of its porosity and average pore diameter. On the other hand, the porosity of the AC series filters decreased with increasing heat treatment temperature, while their average pore diameter increased as the heat treatment temperature increased from 1100 to 1300°C and then drastically decreased at 1400°C. While the porosities of the AC series filters treated at temperatures of up to 1200°C were similar to those of the CN series filter treated at temperatures of up to 600°C, their

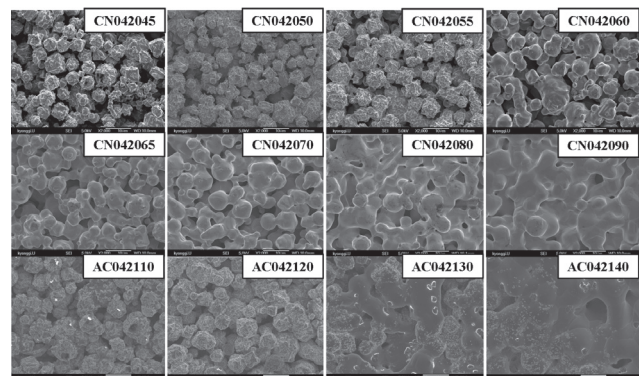


Fig. 2. The surface SEM images of the CN and AC series filters: $\times 2,000$.

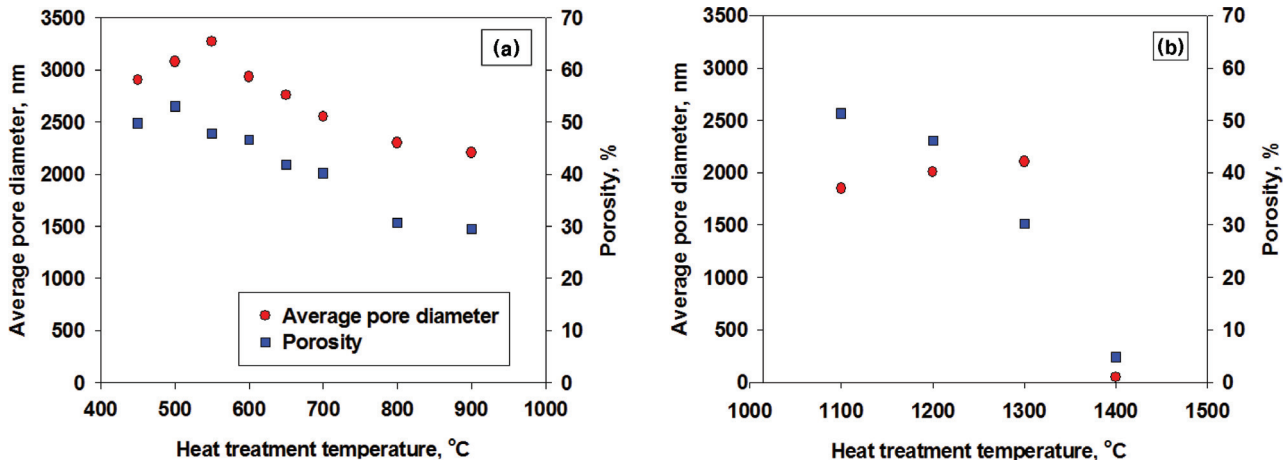


Fig. 3. The porosity and average pore diameter of the CN (a) and AC (b) series filters.

average pore diameters were smaller than those of the CN series filters.

Fig. 4. shows the pore distributions of the CN and AC series filters. The pore distributions were affected by the heat treatment temperature. In the case of the CN series filters, the total pore volumes decreased as the heat treatment temperature increased. While the total volumes of AC042110 and AC042120 were similar to each other, the

total volume of AC042130 treated at 1300°C was much less than those of AC042110 and AC042120.

3.2. Air permeation test

In Fig. 5, the air permeation of the CN (a) and AC (b) series filters are shown as a function of the pressure drop. The air permeations of the CN series filters increased

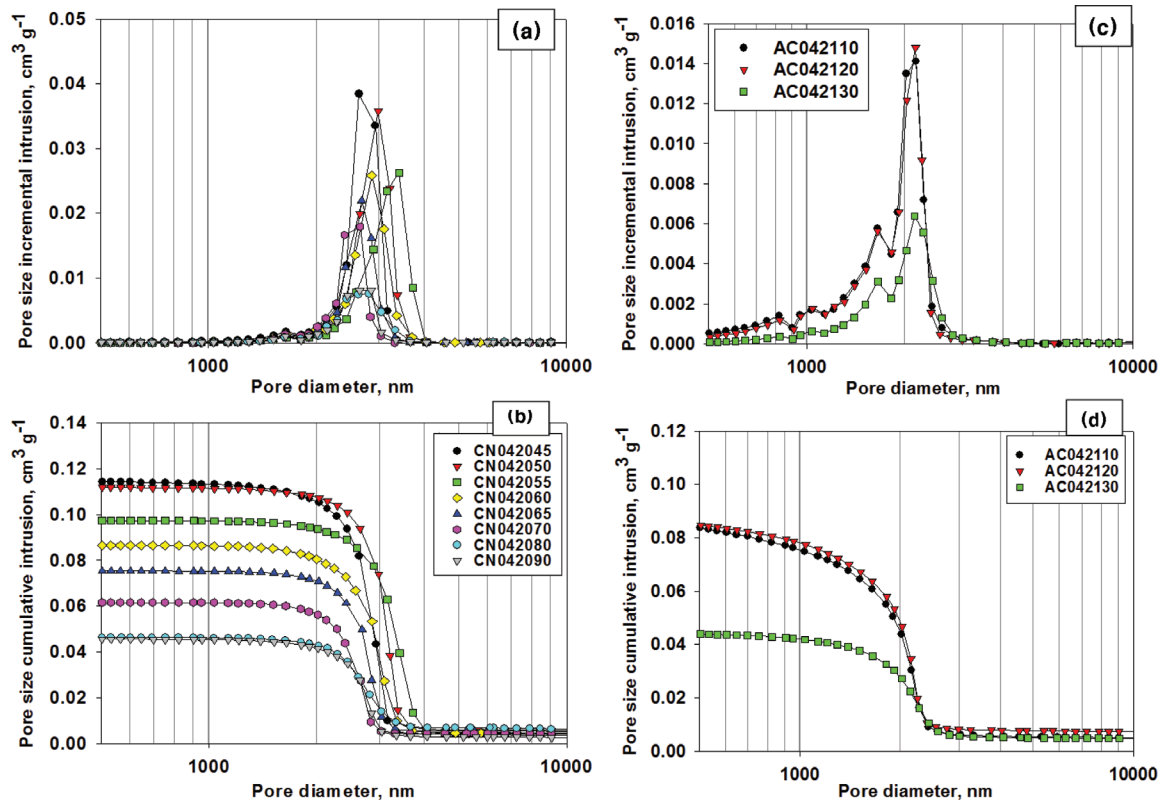


Fig. 4. Pore distributions of CN (a, b) and AC series filters (c, d): (a) and (c) are the incremental intrusion; (b) and (d) are the cumulative intrusion.

linearly with increasing pressure drop. Although the rate of increase of the air permeation (slopes of graph) generally decreased with increasing heat treatment temperature, that of CN042050, i.e., treated at 500°C, was larger than that of CN042045, i.e., treated at 450°C. Except for these two filters, the air permeation fluxes of all of the CN series filters decrease with increasing heat treatment. Above 700°C, their air permeation drastically decreased and the air permeation of CN042900 was approximately half that of CN042800. According to the porosity and average pore diameter analysis in Fig. 3, these filters seem to have similar porosities and pore diameters. However, Fig. 4 shows that CN042800 has a broader pore distribution than CN042900. We can conclude that the broad pore distribution of CN042800 is responsible for its having a higher air permeation flux than that of CN042900.

The air permeation fluxes of the AC series filters in Fig. 5 (b) also increased linearly with increasing pressure drop. The air permeation flux of AC042130 treated

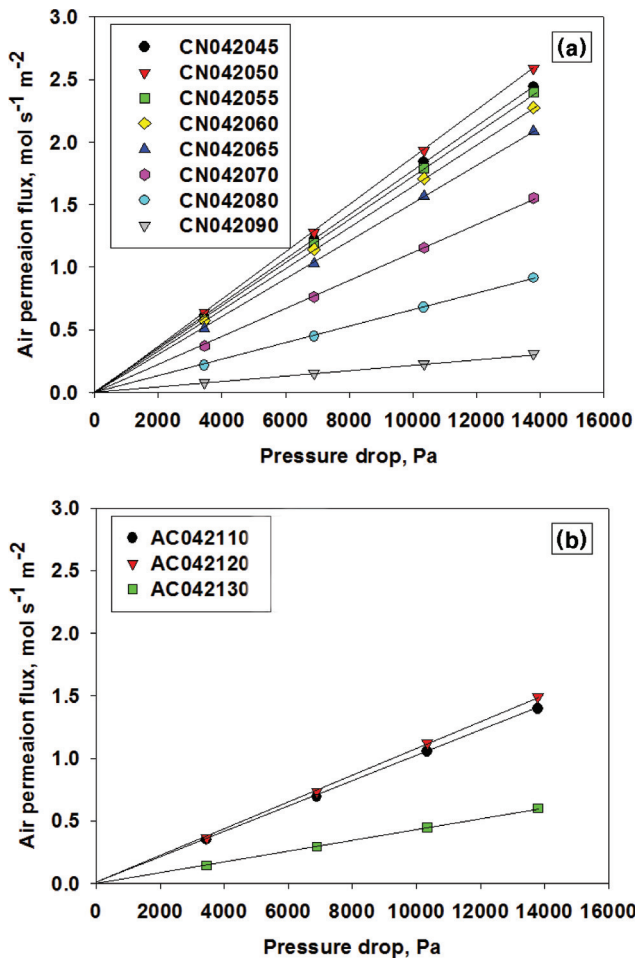


Fig. 5. The air permeation flux as a function of the pressure drop of the CN (a) and AC (b) filters: the test temperature is room temperature.

at 1300°C was much less than those of AC042110 and AC042120. The air permeation flux of AC042120 treated at 1200°C was similar to that of AC042110 treated at 1100°C. This can be explained by their pore distributions shown in Fig. 4 (b). The pore distributions of AC042110 and AC042120 were almost the same.

Fig. 6 (a) shows the effect of the heat treatment temperature on the air permeation flux of the CN series filters. It can be seen that the air permeations of CN042045 and CN042055, which were treated at 450°C and 550°C, respectively, were almost the same. CN042050, which was treated at 500°C, had a higher air permeation flux than CN042045, which was treated at 450°C. This can be explained by the results of the porosity and average pore diameter analysis shown in Fig. 3, where the porosity and average pore diameter of CN042050 are seen to be larger than those of CN042045. Although the air permeation drastically decreased above 700°C, the rate of decrease of the air permeation was relatively small up to a heat treatment temperature of 650°C. This means that the CN series filters can withstand temperatures of up to 650°C.

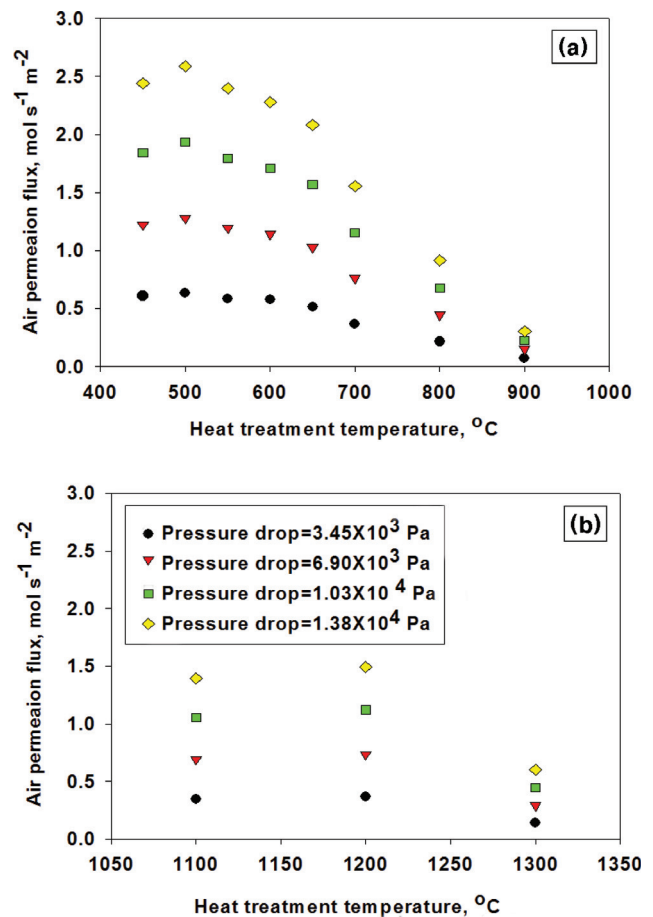


Fig. 6. The air permeation flux as a function of the heat treatment temperature for the CN (a) and AC (b) series filters: the test temperature is room temperature.

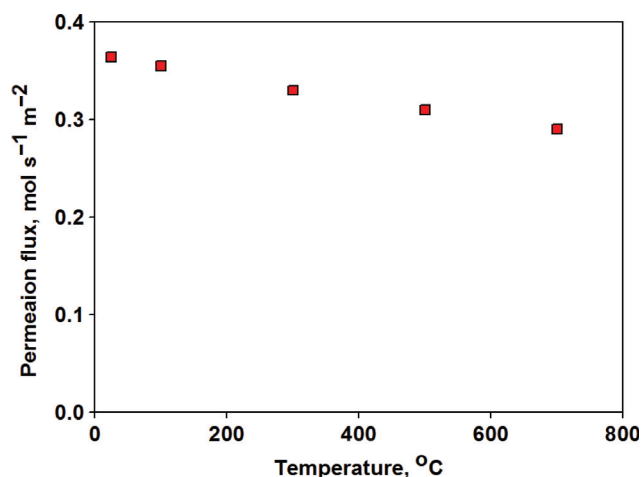


Fig. 7. The air permeation flux as a function of temperature: the filter is AC042120; the pressure drop is 3.44×10^3 Pa.

However, these filters cannot be directly applied to processes demanding very high temperature gas cleaning, such as solid fuel gasification, etc. On the other hand, the results obtained for the AC series filters in Fig. 6 (b) show that the air permeation fluxes of AC042110 and AC042120 were similar to each other. The air permeation flux of AC042130 was higher than that of CN042090. While the average pore size and porosity (Fig. 3) of CN042090 and AC042130 are almost the same, the pore distribution of (Fig. 4) the latter was broader than that of the former and, thus, AC042130 has a higher air permeation flux than CN042090. The air permeation flux of AC042130 was much smaller than those of AC042110 and AC042120.

We performed air permeation tests on the AC042120 filter at different temperatures. Fig. 7 displays the air permeation flux as a function of the operating temperature. The air permeation flux decreased with increasing operation temperature. Its rate of decrease remained almost the same as the viscosity of air increased. From the air permeation test, we can conclude that the alumina modified nickel filter can withstand temperatures of up to 1200°C.

4. Conclusions

An alumina coating was deposited on nickel nano-filters to increase their thermal stability for hot gas cleaning. The average pore diameter, porosity and total pore volume, which strongly affect the air permeation flux, could be controlled by adjusting the fabrication pressure and heat treatment temperature. The SEM, mercury porosimetry and air permeation analyses showed that the alumina coating on the surface of the nickel filters enabled them to withstand temperatures of up to 1200°C.

We believe that the nickel filters developed herein could be applied to high temperature processes, such as solid fuel gasification, not only for the reliable and environmentally sound operation of the subsequent processes, but also to provide energy savings and more effective whole process optimization.

Acknowledgements

This work was supported by a grant from the New and Renewable Energy Research Programs (2008-N-HY-08-9-03-0-000) of the Korea Institute of Energy Technology Evaluation and Planning (KETEP) funded by the Ministry of Knowledge Economy, Republic of Korea.

References

- [1] J.M. Beer, Combustion technology developments in power generation in response to environmental challenges, *Prog. Energ. Combust.*, 26 (2000) 301–327.
- [2] M. Aineto, A. Acosta, J.M. Ricon and M. Romero, Thermal expansion of slag and fly ash from coal gasification in IGCC power plant, *Fuel*, 85 (2006) 2352–2358.
- [3] A. Verma, A.D. Rao and G.S. Samuelsen, Sensitivity analysis of a Vision 21 coal based zero emission power plant, *J. Power Source*, 158 (2006) 417–427.
- [4] A. Mountouris, E. Voutsas and D. Tassios, Solid waste plasma gasification: Equilibrium model development and energy analysis, *Eng. Convers. Manage.*, 47 (2006) 1723–1737.
- [5] D.R. McIlveen-Wright, F. Pinto, L. Armesto, M.A. Caballero, M.P. Aznar, A. Cabanillas, Y. Huang, C. Franco, I. Gulyurtlu and J.T. McMullan, A comparison of circulating fluidized bed combustion and gasification power plant technology for processing mixtures of coal, biomass and plastic waste, *Fuel Process. Technol.*, 87 (2006) 793–801.
- [6] T.-H. Kwak, S. Maken, S. Lee, J.-W. Park, B.-R. Min and Y.D. Yoo, Environmental aspects of gasification of Korean municipal solid waste in a pilot plant, *Fuel*, 85 (2006) 2012–2017.
- [7] R. Maya-Yescas, E.F. Villafuerte-Macias, R. Aguilar and D. Salazar-Sotelo, Sulphur oxides emission during fluidized-bed catalytic cracking, *Chem. Eng. J.*, 106 (2005) 145–152.
- [8] T.J. Campbell, A.H. Shaaban, F.H. Holcomb, R. Salavani and M.J. Binder, JP-8 catalytic cracking for compact fuel processors, *J. Power Source*, 129 (2004) 81–89.
- [9] A. Bayram, A. Muezzinoglu and R. Seyfioglu, Presence and control of polycyclic aromatic hydrocarbons in petroleum coke drying and calcinations plants, *Fuel Process. Technol.*, 60 (1999) 111–118.
- [10] S.E. Pratsinis and P.T. Spicer, Competition between gas phase and surface oxidation of TiCl_4 during synthesis of TiO_2 particles, *Chem. Eng. Sci.*, 53 (1998) 1861–1868.
- [11] M.S. Wooldridge, S.A. Danczyk and J. Wu, Demonstration of gas-phase combustion synthesis of nanosized particles using a hybrid burner, *Nanostruct. Mater.*, 11 (1999) 955–964.
- [12] M. Valix and W.H. Cheung, Study of phase transformation of laterite ores at high temperature, *Miner. Eng.*, 15 (2002) 607–612.
- [13] C. Galassi, Processing of porous ceramics: Piezoelectric materials, *J. Eur. Ceram. Soc.*, 26 (2006) 2951–2958.
- [14] J. Oi-Uchisawa, S. Wang, T. Nanba, A. Ohi and A. Obuchi, Improvement of Pt catalyst for soot oxidation using missed oxide as a support, *Appl. Catal. B: Environ.*, 44 (2003) 207–215.
- [15] K. Yoshikawa, R&D (Research and Development) on distributed power generation from solid fuels, *Energy*, 31 (2006) 1656–1665.
- [16] C.D. Chang, W.H. Lang and A.J. Silvestri, Synthesis gas conversion to aromatic hydrocarbons, *J. Catal.*, 56 (1979) 268–273.

- [17] Q. Zhang, X. Li, K. Asami, S. Asaoka and K. Fujimoto, Synthesis of LPG from synthesis gas, *Fuel Process. Technol.*, 85 (2004) 1139–1150.
- [18] M. Ni, D.Y.C. Leung, M.K.H. Leung and K. Sumathy, An overview of hydrogen production from biomass, *Fuel Process. Technol.*, 87 (2006) 461–471.
- [19] G. Iaquaniello and A. Mangiapane, Integration of biomass gasification with MCFC, *Int. J. Hydrogen Energy*, 31 (2006) 399–404.
- [20] F. Engstrom, Hot gas clean-up bioflow ceramic filter experience, *Biomass Bioenergy* 15, (1998) 259–262.
- [21] L. Armesto and J.L. Merino, Characterization of some coal combustion solid residues, *Fuel*, 78 (1999) 613–618.
- [22] W. de Jong, O. Unal, J. Andries, K.R.G. Hein and H. Spliethoff, Biomass and fossil fuel conversion by pressurized fluidized bed gasification using hot gas ceramic filters as gas cleaning, *Biomass Bioenergy*, 25 (2003) 59–83.
- [23] A. Larbot, M. Bertrand, S. Marre and E. Prouzet, Performances of ceramic filters for air purification, *Sep. Purif. Technol.*, 32 (2003) 81–85.
- [24] N.L. de Freitas, J.A.S. Goncalves, M.D.M. Innocentini and J.R. Coury, Development of a double-layered ceramic filter for aerosol filtration at high-temperature: The filter collection efficiency, *J. Hazard. Mater.*, 2006 (136) 747–756.
- [25] E. Schmidt, P. Gang, T. Pilz and A. Dittler, High temperature gas cleaning, *Institut für Mechanische Verfahrenstechnik und Mechanik der Universität Karlsruhe*, 1996.
- [26] S.-K. Ryi, J.-S. Park, S.-J. Park, D.-G. Lee and S.-H. Kim, Fabrication of nickel filter made by uniaxial pressing process for gas purification: fabrication pressure effect, *J. Membr. Sci.*, 299 (2007) 174–180.